Polymer Chemistry

ROYAL SOCIETY OF CHEMISTRY

PAPER

View Article Online
View Journal | View Issue

Cite this: *Polym. Chem.*, 2023, **14**, 952

New long-wavelength D–π-A–π-D chalcone photoinitiator for visible light polymerization with photobleaching and biocompatibility properties†

Yanyang Gao and Jinqing Qu *

Four chalcones with large conjugated structures have been designed and synthesized. The large conjugated structures of the four chalcones give them excellent absorption properties in the visible region (λ_{max} = 407–483 nm, ε_{max} = 24600–60200 M^{-1} cm^{-1}) and excellent intramolecular charge transfer characteristics. After forming a three-component photoinitiation system with iodine and an amine, the free radical polymerization of various acrylates was effectively initiated under UV-LED and blue LED irradiation, with a final double bond conversion rate of 92%. The photochemical reaction mechanism was determined using steady-state photolysis, fluorescence quenching, cyclic voltammetry and ESR experiments. In addition, the chalcones were found to have good photobleaching properties and biocompatibility through photoinduced degradation and cytotoxicity experiments. These excellent properties demonstrate that these chalcones have great promise for applications in the field of photopolymerization.

Received 28th December 2022,
Accepted 18th January 2023

DOI: 10.1039/d2py01601j

rsc.li/polymers

1. Introduction

Photopolymerization refers to the process of crosslinking monomers and resins to form solid products in the presence of light,[1–4] and it is widely used in many materials science fields because of its high efficiency and wide adaptability.[5,6] The mercury lamp that serves as the UV light source in traditional photopolymerization technology has some safety problems, such as causing damage to human eyes and skin, and ozone and mercury pollution generated by the polymerization process.[7–10] Therefore, in recent years, more and more attention has been paid to lower energy and soft visible irradiation sources such as LEDs, which can not only avoid safety problems, but also prevent deformation of materials at lower operating temperatures.[11–14]

At present, the maximum absorption wavelength of free radical initiators on the market, such as photoinitiator 1173 and benzophenone, is below 365 nm, but the wavelength of LED light sources widely used in the industrial field is above 365 nm. Thus, this mismatch between the LED wavelength and the initiator absorption wavelength means that there is low initiation efficiency or that the LEDs cannot be used.[15,16] Commercial photoinitiators with absorption wavelengths greater than 365 nm, such as trimethylbenzoyl diphenylphosphine oxide (TPO), produce harmful free radicals in the photopolymerization process and have been banned under EU regulations. To solve this problem, it is necessary to develop a green non-toxic photoinitiator with an absorption wavelength that sufficiently matches the wavelength emitted by the light source. One of the main strategies to achieve this is to increase the size of the conjugated structure of the molecule to improve its absorption properties so that the absorption wavelength is red-shifted and it has a high molar extinction coefficient.[17]

In recent years, photoinitiators based on natural dyes such as curcumin,[18] flavonoids,[19] carotenoids,[20] and anthocyanins[21] have gained widespread attention due to their availability, low cost, and green non-toxic properties. Chalcones are type of natural dye that also exist in many plants, and chalcone-based photoinitiators are easily accessible and have good light absorption performance in the near-ultraviolet-visible region. Chalcones also have an ideal structure for designing visible light photoinitiators to induce photopolymerization reactions,[22] while chalcone-based photoinitiators have good photobleaching properties and good biocompatibility, making them suitable for a wide range of applications in 3D printing and dental materials.[23]

Triphenylamine (TPA) is one of the most widely used electron donors in the fields of organic light-emitting materials and light-induced color-changing materials.[24–27] The introduction of TPA groups into photoinitiators to form D–π-A structures enhances intramolecular charge transfer (ICT) effects, resulting in strong transitions in the visible region. This

School of Chemistry and Chemical Engineering, South China University of Technology, Guangzhou, Guangdong, 510641, People's Republic of China. E-mail: cejqqu@scut.edu.cn

† Electronic supplementary information (ESI) available. See DOI: https://doi.org/10.1039/d2py01601j

enables the photoinitiator to have excellent absorption properties.[10,28] Fluorene is a commonly used raw material and intermediate for organic synthesis, and is widely used in pharmaceuticals, dyes and various polymer preparations.[29] Its rigid planar structure is similar to that of biphenyl but gives it better thermal stability and light-induced luminescence efficiency, making it favored for the design of luminescent materials. Lalevee and coworkers designed and synthesized several chalcones that contain triphenyl amine and have high polymerization efficiency for free radical polymerization under 405 nm LED irradiation.[30] Chen and his colleagues synthesized a series of TPA-based conjugated chalcone structures with intense absorption bands and high molar extinction coefficients at around 405 nm.[31] Fu and his coworkers synthesized two TPA-based chalcones for the deep curing of resin and ceramic suspensions.[32]

In our previous studies, we synthesized two phenothiazine photoinitiators with a maximum absorption wavelength of 440 nm.[33] On a similar basis, in this work, two kinds of triphenylamine photoinitiators and two kinds of fluorene photoinitiators were synthesized as free radical photoinitiators. In the presence of LED illumination and sunlight, the photoinitiation activity of trimethylolpropane triacrylate (TMPTA) polymerization was studied and the optical, electrochemical, and theoretical properties were investigated. In addition, cytotoxicity experiments were performed on HeLa cells (Scheme 1).

2. Results and discussion

2.1 UV-vis absorption spectrum

The absorption spectra of the chalcones in dimethyl sulfoxide (DMSO) is shown in Fig. 1(a). Compared with TPAK, the four

Table 1 Photophysical properties of the chalcones

Sample	TPAK	TPA-1	TPA-2	DFO-1	DFO-2
λ_{max} (nm)	430	478	483	407	458
ε_{max} (M^{-1} cm^{-1})	27 500	57 500	60 200	24 600	53 900

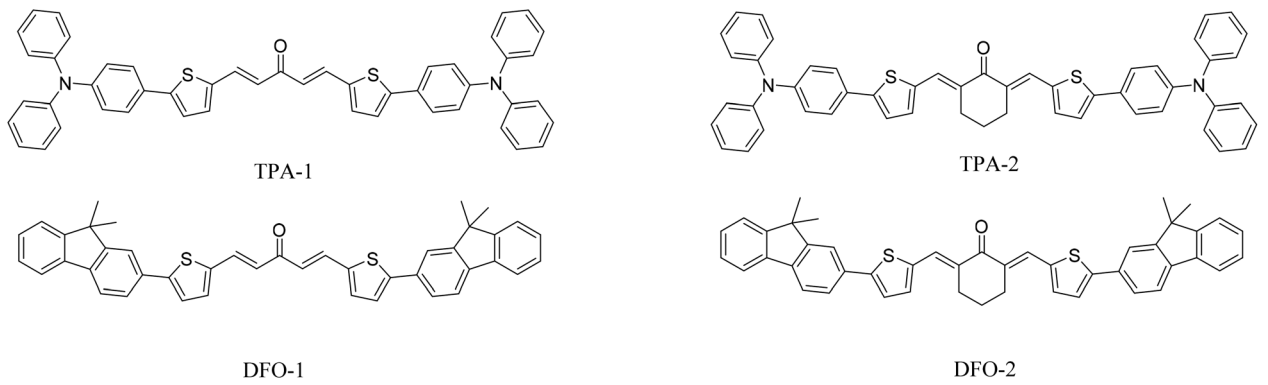

Scheme 1 Chemical structures of the chalcones examined in this study.

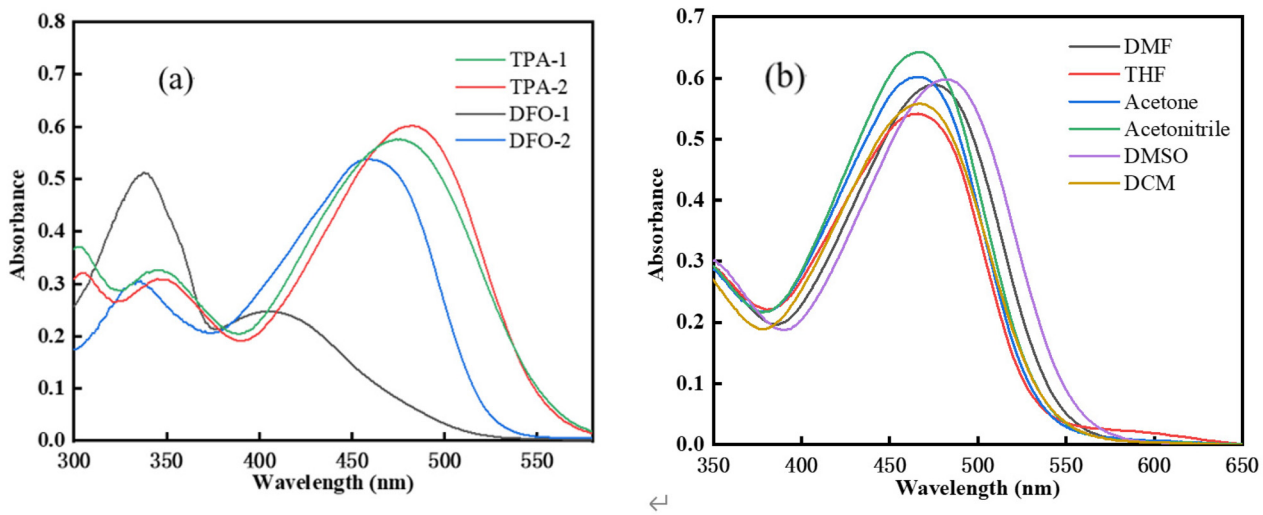

Fig. 1 (a) Absorption spectra of the chalcones ($c = 1 \times 10^{-5}$ mol L^{-1}). (b) TPA-2 absorption peaks in different solvents.

Table 2 Light absorption properties of TPA-2

Solvent	DMSO	DMF	ACN	Acetone	THF	DCM
λ_{max} (nm)	483	477	470	469	468	467
ε_{max} (M^{-1} cm^{-1})	60 200	58 900	64 100	60 100	53 900	55 700

chalcones were found to have absorption bands with a considerable molar extinction coefficient in the visible light region,[32] indicating that a large conjugated D–π-A–π-D structure could make the absorption peak redshift. The photophysical properties of the chalcones are shown in Table 1. It should be pointed out that (1E,4E)-1-(5-(9,9-dimethyl-9,9a-

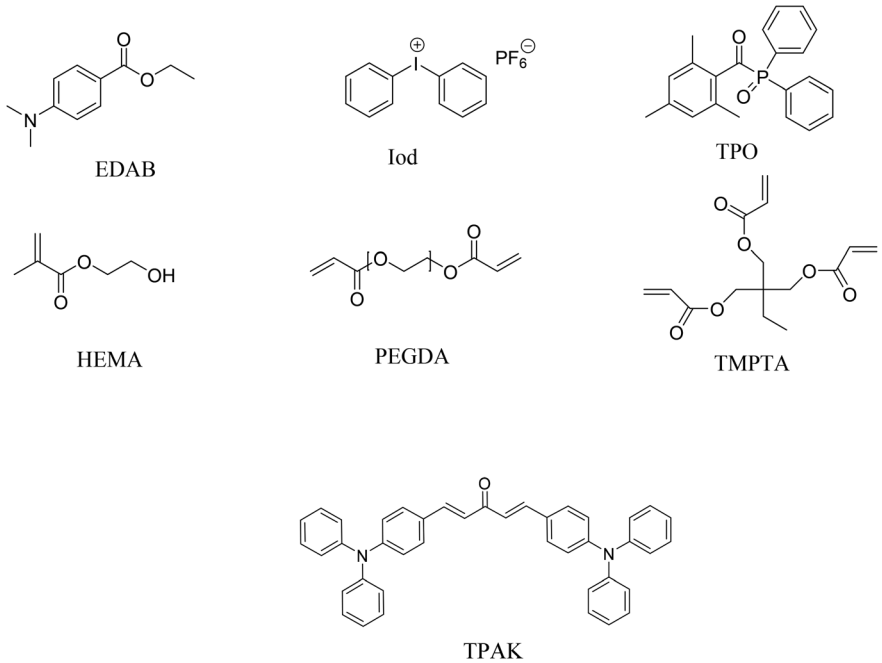

Scheme 2 Chemical structures of the other compounds used in this study.

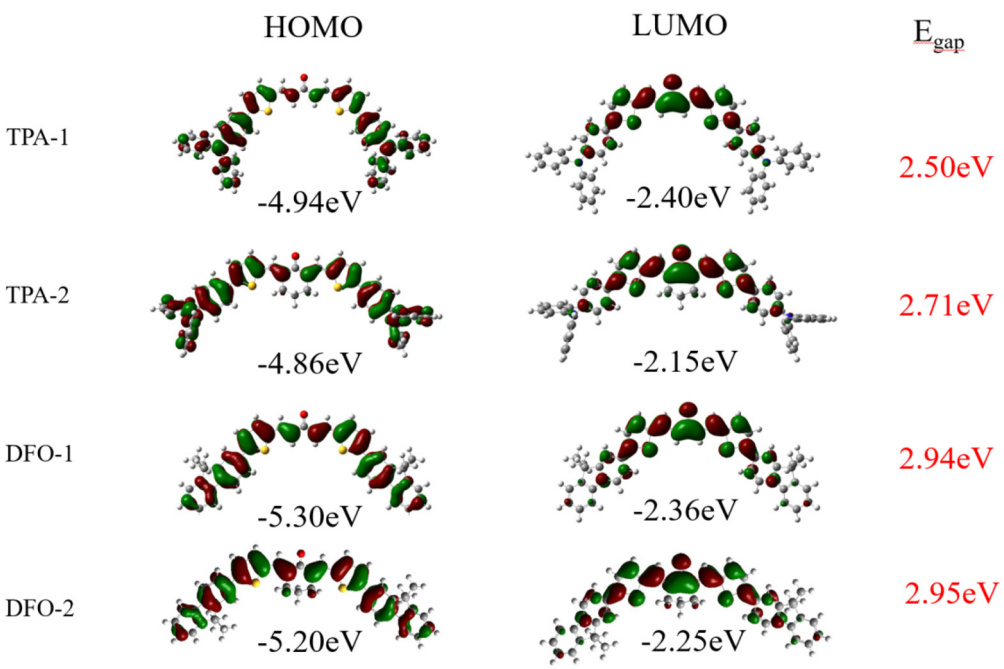

Fig. 2 HOMOs and LUMOs of the chalcones.

dihydro-4aH-fluoren-7-yl)thiophen-2-yl)-5-(5-(9,9-dimethyl-9H-fluoren-3-yl)thiophen-2-yl)penta-1,4-dien-3-one has a very different absorption wavelength from the other chalcones, which may be attributed to its flat structure. The effect of different solvents on the absorption peak of TPA-2 is shown in Fig. 1(b) and Table 2. It can be seen that as the solvent polarity increases, the absorption peak undergoes a redshift, although not an obvious redshift, which might be due to the symmetrical structure of TPA-2. The absorption intensity of the peak also changed, which might be attributed to the change in the solubility of TPA-2 in different solvents. In addition, the π–π* transition of the large conjugate structure of the molecule might extend the absorption wavelength range to 600 nm.[34] The high molar extinction coefficient and wide absorption spectrum of these four chalcones indicates that they have great potential in the field of photopolymerization (Scheme 2).

Fig. 2 shows the HOMOs and LUMOs of the chalcones. The lowest energy state of the modeled geometry was obtained from optimization calculations. In addition to the typical π–π* transition behavior, the HOMO–LUMO transitions exhibited intramolecular charge transfer (ICT) characteristics. The ground state electron density was principally distributed over the entire molecule, while the electron density of the LUMO was mainly localized on the vinyl and carbonyl groups. This

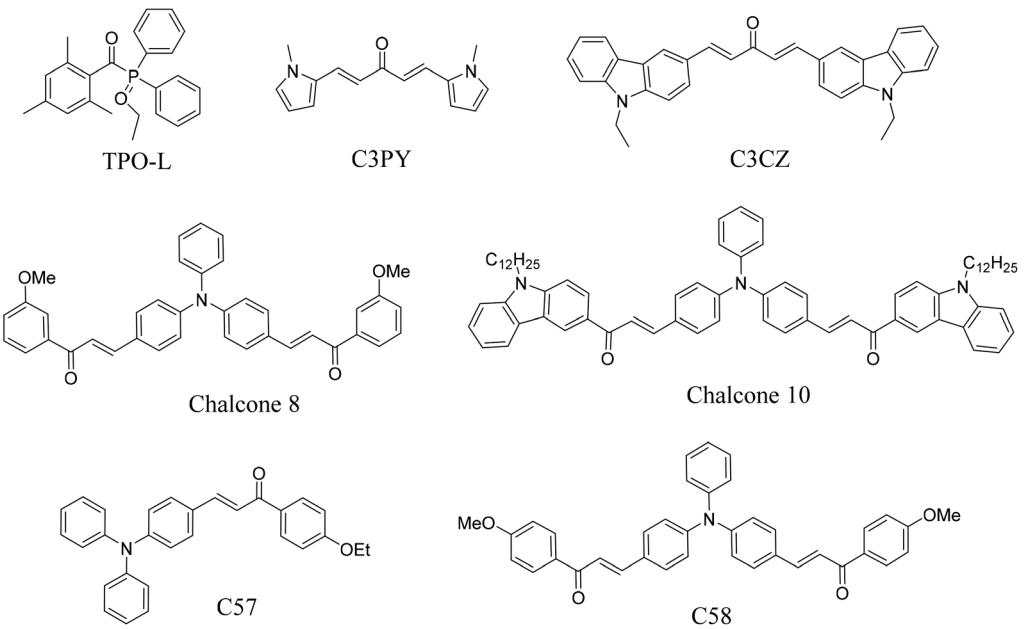

Scheme 3 Chemical structures of other photoinitiators listed in Table 6.

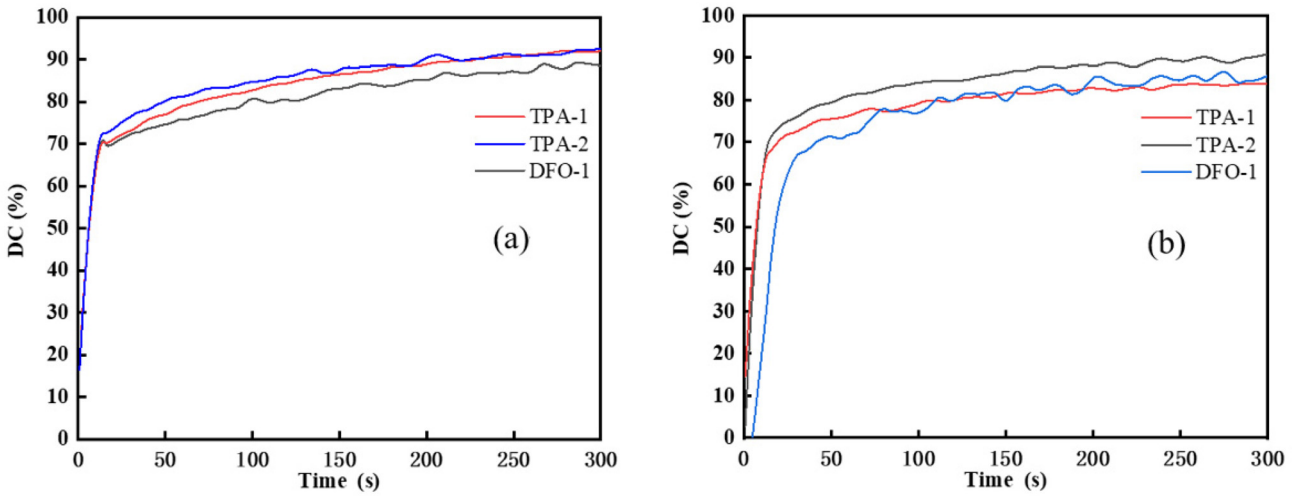

Fig. 3 Photopolymerization kinetics of the chalcones/Iod/EDAB systems (chalcones: 0.1 wt%; Iod: 1.0 wt%; EDAB: 1.0 wt%, TMPTA as monomer) under different light sources (a) 365 nm LED, (b) 405 nm LED.

Table 3 Curing times under different conditions

No.	TPA (wt%)	Iod (wt%)	EDAB (wt%)	TMPTA (wt%)	365 (s)	480 (s)	Solar (s)
1	0.1	—	—	99.9	310	280	310
2	—	2	—	98	Uncured		
3	—	—	2	98	Uncured		
4	0.1	—	1	99	210	180	180
5	0.1	—	2	98	180	120	150
6	0.1	1	—	99	10	6	6
7	0.1	2	—	98	8	4	5
8	0.1	1	1	98	5	3	3

Table 4 Curing times with different monomers

No.	TPA (wt%)	Iod (wt%)	EDAB (wt%)	Monomer	365 (s)	480 (s)	Solar (s)
1	0.1	1	1	HEMA	310	280	310
2	0.1	1	1	PEGDA	10	8	8
3	0.1	1	1	TMPTA	5	3	3

ICT phenomenon indicates that the chalcones have a D–π-A–π-D structure. Consistent with the experimental results, the band gap of the TPA series is smaller than that of the DFO series, indicating that the TPA group has a stronger electron-donating ability, reduced the ionization potential energy of the molecule, and giving it a longer absorption wavelength (Scheme 3).

2.2. Photopolymerization kinetic investigations of the chalcones

The influence of different wavelength light sources on the photopolymerization reaction was investigated, and 365 nm and 405 nm LED light sources commonly used in industry were used to compare the photopolymerization performance. The DFO-2/ethyl 4-(dimethylamino)benzoate (EDAB); diphenyliodonium hexafluorophosphate (Iod) system was not tested due to its poor solubility in TMPTA, and the results are shown in Fig. 3.

As shown in Fig. 3(a), under illumination with the 365 nm light source, the double bond conversion could reach 70% for

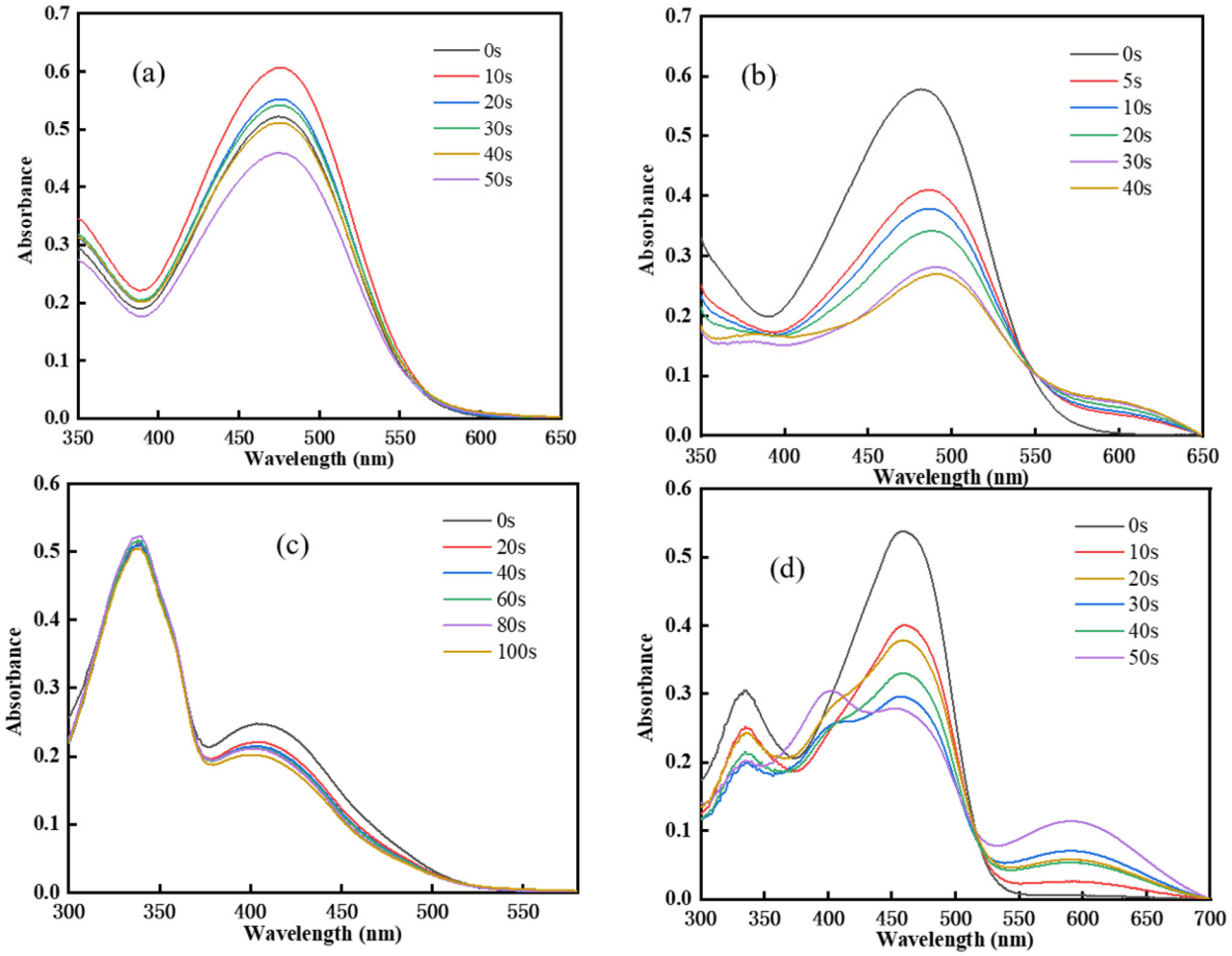

Fig. 4 Steady state UV degradation of chalcones: (a) TPA-1/Iod; (b)TPA-2/Iod; (c) DFO-1/Iod; (d) DFO-2/Iod.

the chalcones/Iod/EDAB systems after 15 s irradiation time. Although the molar absorption coefficient of DFO-1 at 365 nm was greater than that of TPA-1 and TPA-2, their final double bond conversion values were similar, 91%, 92% and 88%, respectively. This might be due to the faster reaction rate between TPA-1 and TPA-2 and Iod. Under illumination with the 405 nm light source, the double bond conversion rate of DFO-1 decreased more, which might be attributed to the obvious reduction of its molar extinction coefficient at 405 nm. However, the double bond conversion of the chalcones/Iod/EDAB systems still reaches more than 84%, indicating that the chalcones/Iod/EDAB system has excellent photoinitiation efficiency.

2.3. Curing time of the coating

The curing time of the coating is an important factor in industrial applications. Therefore, the effects of the light source, monomer, TPA-2, and Iod and EDAB content on curing time were investigated. The results are shown in Table 3, and when only TPA-2 was added the curing time exceeded 300 s, whilst when only Iod or EDAB was added the coating cannot be cured. The curing time was shortened to 6 s and 4 s after adding 1% or 2% Iod. The addition of EDAB does not significantly shorten the curing time of the film, but the addition of the TPA-2/Iod/EDAB system could shorten the curing time of the film to 5 s. In addition, the curing time was also different under illumination with different light sources. The curing time when using the 480 nm light source and sunlight was faster than when the 365 nm light source was used, which might be attributed to the higher molar absorbance of TPA-2 at 480 nm. Table 4 illustrates that the curing rate with the TMPTA and poly(ethylene glycol) diacrylate (PEGDA) monomers is much higher than that with (hydroxyethyl)methacrylate (HEMA).

2.4. Steady state photolysis of chalcones and photobleaching

To monitor the changes in the Chalcones/Iod interactions, the photolysis process was explored, and the absorption spectrum changes as a function of irradiation time are shown in Fig. 4. As the irradiation time increased, the maximum absorption

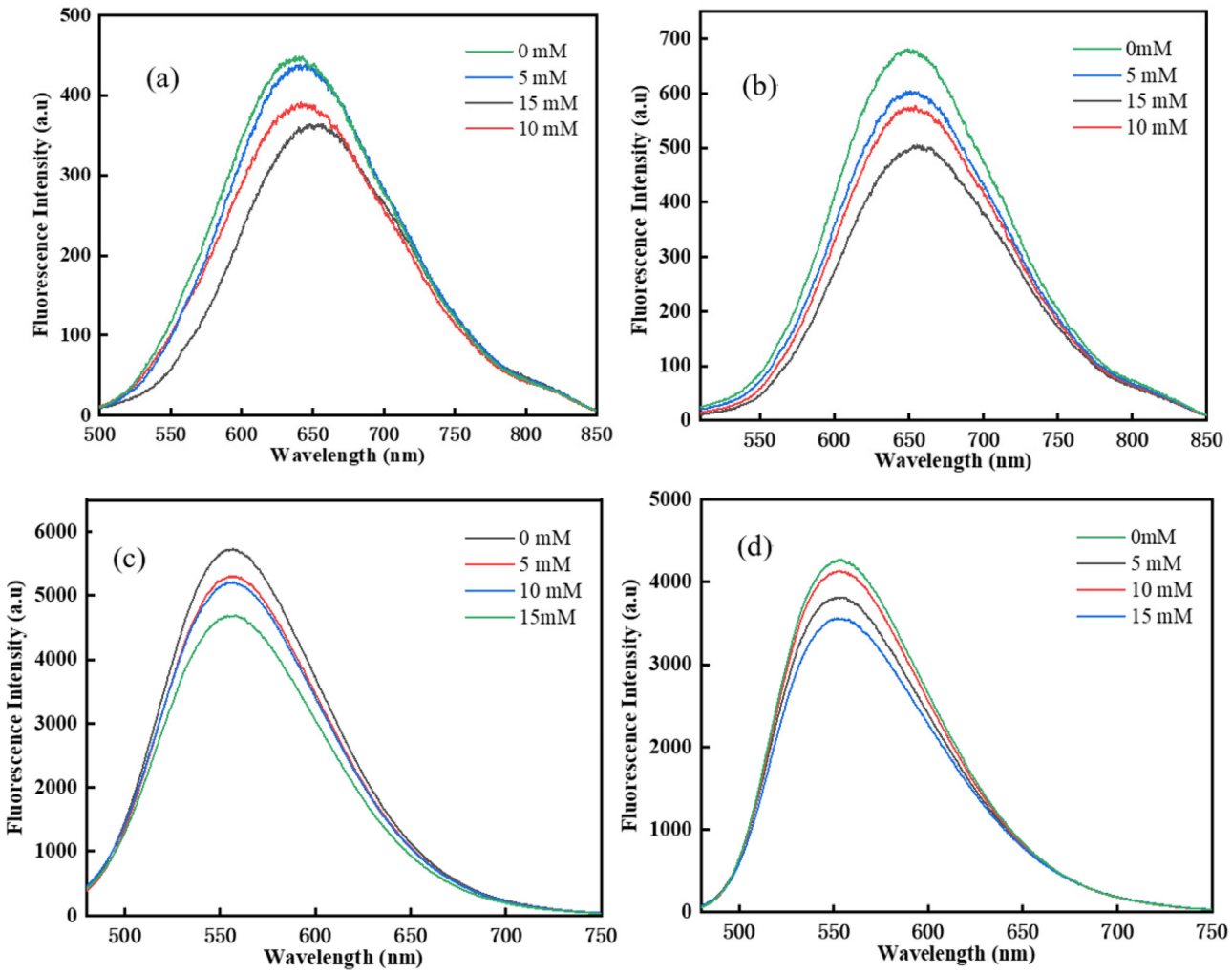

Fig. 5 Fluorescence quenching experiments for the chalcones/Iod systems: (a) TPA-1; (b)TPA-2; (c) DFO-1; (d) DFO-2.

wavelength of the chalcones gradually decreased. It can be seen from Fig. 4(a)–(c) that no new peaks appear in the steady state photolysis process of TPA-1 and DFO-1. In contrast, TPA-2 and DFO-2 have a new peak at 600 nm, indicating that there might be a new substance formed, and the degradation rate was also faster, which might be attributed to their better light absorption performance.

The photobleaching properties of the initiators are effective with colorless or light-colored coatings, and combined with long-wave LED light, they are expected to be used in 3D printing technology. For this purpose, the photobleaching performance of the chalcones in cured coatings was studied, as shown in Fig. S9.† The colors of the chalcones are red and yellow. After LED irradiation for curing, the coating color became lighter, indicating that the chalcones have photobleaching properties.

2.5. Fluorescence and cyclic voltammetry experiments

Fluorescence quenching experiments were carried out in DMSO to further study the photochemical reaction between chalcone and Iod.[35] As shown in Fig. 5, the fluorescence intensity of all four chalcones decreased significantly as the Iod content increased. There were no new peaks in the emission spectrum, which excluded the formation of exciton complexes. This result illustrates that an efficient reaction occurred between the four chalcones and Iod, which might be because of the efficient transfer of photoinduced electrons from the excited state of the chalcones to the ground state Iod.

The electrochemical performance is of great significance for evaluating the feasibility of photoelectron transfer reactions and the redox reversibility of the metal or metal-free photocatalysts.[36] Through the intersection between the UV-vis absorption and fluorescence spectra in DMSO (Fig. S10†), the first singlet excited state energy of the chalcones (ES1 = 2.25 eV for TPA-1, 2.24 eV for TPA-2, 2.45 eV for DFO-1, 2.44 eV for DFO-2) was determined. The cyclic voltammograms (CV) are shown in

Table 5 Electrochemical data for the chalcones

Chalcones	TPA-1	TPA-2	DFO-1	DFO-2
E_{OX} (V)	2.25	2.24	2.45	2.44
E_{S1} (eV)	0.53	0.56	1.56	1.56
ΔG_{et} (eV)	−1.52	−1.48	−0.69	−0.68

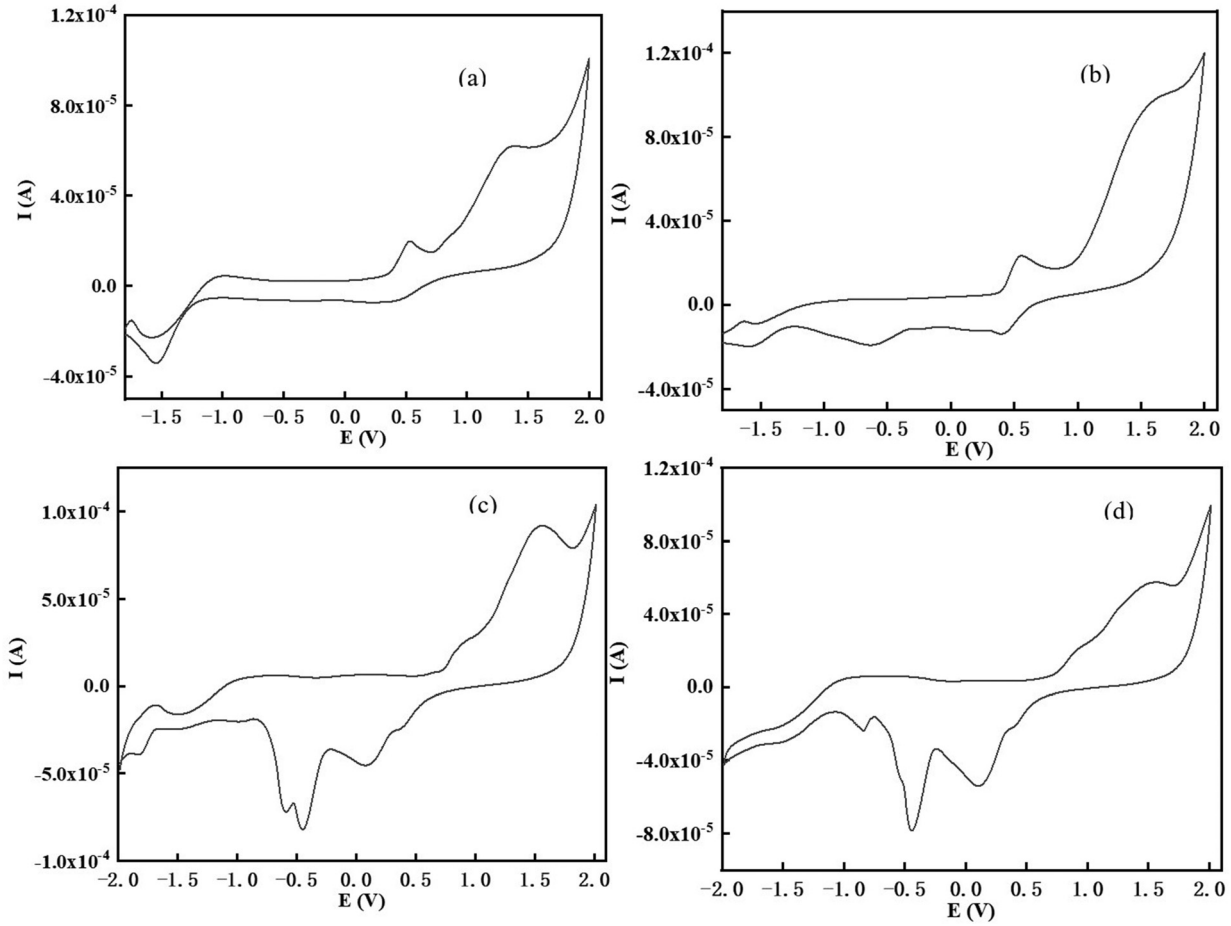

Fig. 6 Cyclic voltammograms of the chalcones in DCM against saturated calomel electrode (SCE) under a nitrogen saturated atmosphere, (a) TPA-1; (b)TPA-2; (c) DFO-1; (d) DFO-2.

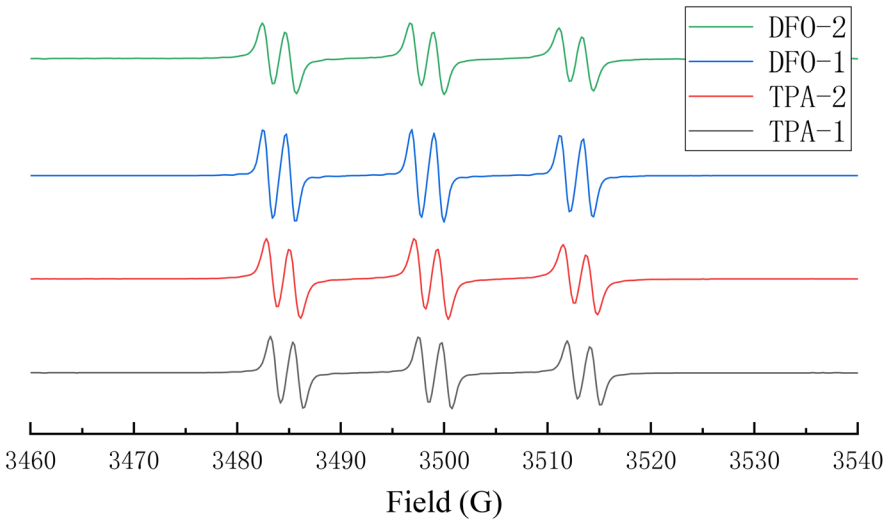

Fig. 7 Electron spin resonance spin trapping spectra of the chalcones/Iod systems.

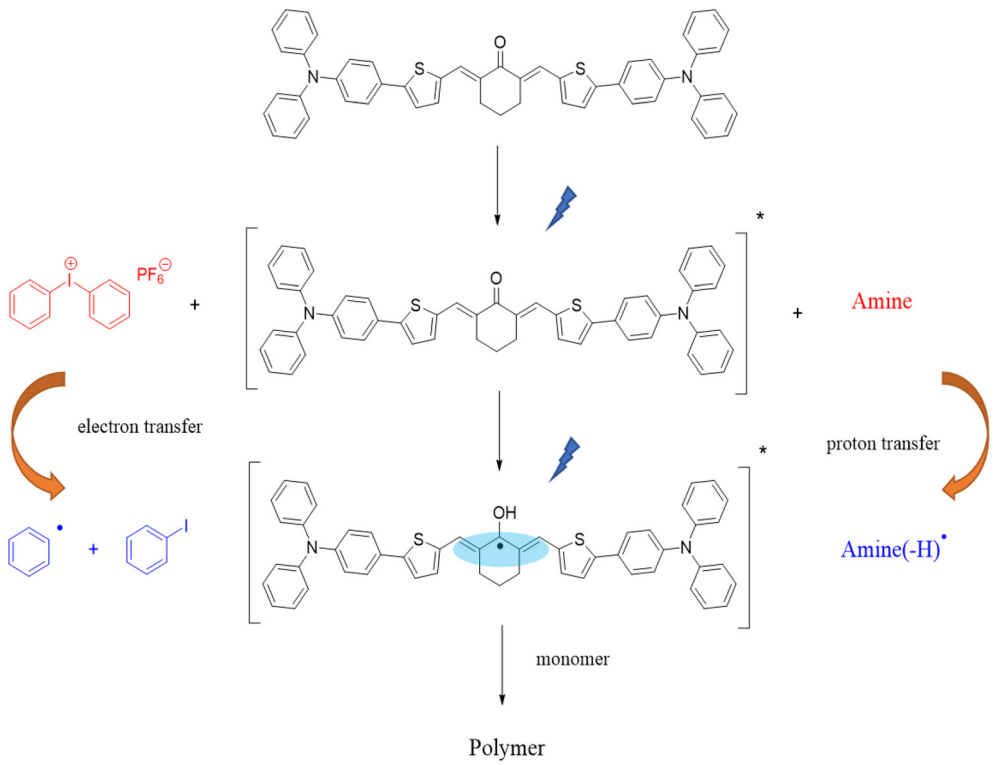

r_1 chaclone $\longrightarrow$ chaclone *

r_2 chaclone * + Iod $\longrightarrow$ chaclone $^{\bullet+}$ + PhI + Ph $^\bullet$

r_3 chaclone * + EDAB $\longrightarrow$ chaclone $^{\bullet-}$ + EDAB $^{\bullet+}$ $\longrightarrow$ chaclone-H $^\bullet$ + EDAB$_{(-H)}^\bullet$

r_4 chaclone $^{\bullet+}$ + EDAB $\longrightarrow$ chaclone + EDAB $^{\bullet+}$

r_5 chaclone-H $^\bullet$ + Iod $\longrightarrow$ chaclone + Ph $^\bullet$ + PhI + H^+

Fig. 8 Proposed photopolymerization mechanisms for TPA-2 and the chalcones.

Fig. 6, and the stronger donating ability of TPA might result from their electron-rich nitrogen atoms.

The calculation results based on the electrochemical data are shown in Table 5, and the ΔG_{et} of all four chalcones is below 0, which indicates that there is a good thermodynamic drive after photoexcitation to allow electrons to transfer between the excited state molecules and Iod. At the same time, the TPA series has a smaller ΔG_{et} than the DFO series, indicating that TPA could undergo a more efficient redox reaction with Iod, thus the rate of action with Iod was faster.

2.6. The photopolymerization mechanism of the chalcones

In order to further understand the mechanism of action of the chalcones in the photopolymerization process, in an N_2 atmosphere, phenylbutylnitrone was used as a free radical trap to study the free radicals generated by the chalcones after LED irradiation. The signal obtained is shown in Fig. 7, and it can be seen that there are obvious and similar radical signals for all the chalcones. The hyperfine coupling constants are aN = 14.5 G and aH = 2.2 G, indicating that the chalcones/Iod system could generate phenyl radicals.[37,38]

Based on the above research and other relevant research,[32,37] we propose a possible experimental mechanism, as shown in Fig. 8. First, under LED illumination, the chalcone absorbs photons to transition to the excited state, which could trigger monomer polymerization but with low efficiency. After adding Iod, the excited state chalcones quickly undergo a single electron transfer reaction with Iod to form phenyl radicals, which trigger the free radical polymerization of the acrylates, thereby improving the initiation efficiency. This mechanism of initiation is also consistent with the experimental results. The addition of EDAB as a hydrogen donor coinitiator enhances the absorption of light by the photoinitiation system,[39] and the interaction between the chalcones and EDAB forms active free radicals, which in turn trigger the free radical polymerization.

2.7. Cellular cytotoxicity

With the application of photoinitiators in food packaging, biomedicine, and 3D printing, it is important to evaluate the biocompatibility of the photoinitiators. Cytotoxicity was tested using MTT colorimetry over a concentration gradient of 10 μM to 50 μM and compared to the industrial photoinitiator TPO. The results are shown in Fig. 9 and show that, compared with TPO, the four chalcones have no significant reduction in cell viability. The cell survival rate of the TPA series is maintained at more than 89% when the concentration is increased to 50 μM, and the cell survival rate of the DFO series is also maintained at more than 85%. These results are significantly better than those obtained when using TPO, indicating that the four synthesized chalcones had good biocompatibility with cells, thus broadening their range of industrial applications.

2.8. Comparison with other photoinitiators

The chalcones were compared with TPO and other photoinitiators and the results are shown in Table 6. The molar absorption coefficients of the photoinitiators TPA-1, TPA-2, and DFO-2 were 57 500, 60 200, and 53 900, respectively, 100 times that of TPO. At the same time, compared with other bis chalcone photoinitiators, the photoinitiators synthesized in this paper had longer absorption wavelengths and larger molar absorption coefficients. With the help of coinitiators, the double bond conversion performance with 0.1 wt% TPA-1, TPA-2, and DFO-1 could reach 89%. The comparison results also show that the photoinitiators synthesized in this paper have excellent light absorption properties and could be used in industrial fields.

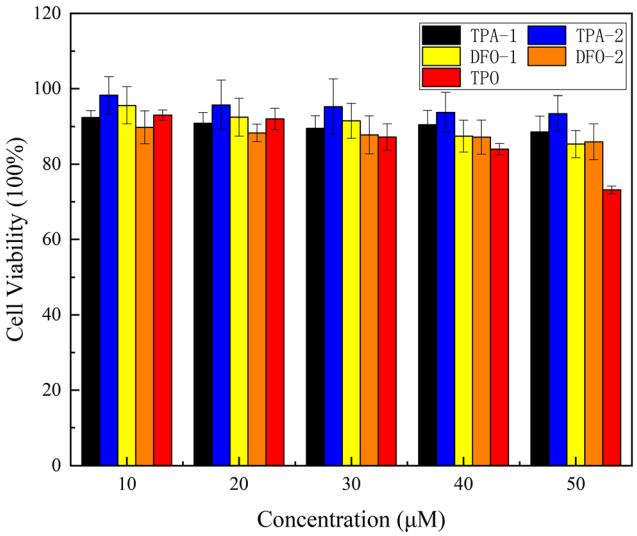

Fig. 9 Viability of HeLa cells co-cultured with the chalcones and TPO for 24 h.

Table 6 Comparison of the photoinitiators synthesized in this paper with other photoinitiators

PI	λ_{max} (nm)	ε_{max} (L mol^{-1}) cm^{-1}	Content (wt%)	DC (%)	Ref.
TPO	380	591	2	58	40
TPO-L	383	131	4	57	41
TPAK	430	27 500	0.1	60	32
C3PY	413	43 300	0.1	78	42
C3CZ	403	40 090	0.1	87	42
Chalcone 8	430	7990	1.5	55	37
Chalcone 10	430	10 500	1.5	85	37
C57	411	17 500	1	30	23
C58	428	8540	1.5	85	43
TPA-1	478	57 500	0.1	91	This study
TPA-2	483	60 200	0.1	92	This study
DFO-1	407	24 600	0.1	89	This study
DFO-2	458	53 900	0.1	––	This study

3. Conclusions

In this article, four chalcones with large conjugated structures were reported. Their large conjugated structures enhanced the intramolecular charge transfer effect, giving them excellent light

absorption properties in the visible region. The maximum absorption wavelength of one of the chalcones based on triphenylamine reached 483 nm, and the maximum molar absorbance coefficient reached 60 200 M^{-1} cm^{-1}. The photopolymerization mechanism was studied using steady-state photolysis, fluorescence quenching, cyclic voltammetry and electron spin resonance experiments, which proved that there was a good interaction between the chalcones and the substrate (Iod) for the promotion of the free radical polymerization of acrylate. After forming a three-component photoinitiation system with Iod and ethyl 4-(dimethylamino)benzoate, the polymerization of Trimethylolpropane triacrylate could be triggered within 10 s, and the final double bond conversion rate was 92%. At the same time, the chalcones showed good photobleaching performance under LED irradiation, and cytotoxicity experiments also proved that the chalcones have good biocompatibility. Given their excellent properties, the chalcones synthesized in this study will have a wide range of applications in industry.

Conflicts of interest

The authors declare that they have no known competing financial interests or personal relationships that could have appeared to influence the work reported in this paper.

Acknowledgements

This work was financially supported by the National Key Research and Development Program of China (2022YFB3806404), the National Natural Science Foundation of China (No. 21878109), and the Science and Technology Program of Guangdong Province, China (No. 2020B1212070027).

References

1 S. Shanmugam, J. Xu and C. Boyer, Light-Regulated Polymerization under Near-Infrared/Far-Red Irradiation Catalyzed by Bacteriochlorophyll a, *Angew. Chem., Int. Ed.*, 2016, **55**(3), 1036–1040.
2 C. Kutahya, C. Schmitz, V. Strehmel, Y. Yagci and B. Strehmel, Near-Infrared Sensitized Photoinduced Atom-Transfer Radical Polymerization (ATRP) with a Copper(II) Catalyst Concentration in the ppm Range, *Angew. Chem., Int. Ed.*, 2018, **57**(26), 7898–7902.
3 A. H. Bonardi, F. Dumur, T. M. Grant, G. Noirbent, D. Gigmes, B. H. Lessard, J. P. Fouassier and J. Lalevée, High Performance Near-Infrared (NIR) Photoinitiating Systems Operating under Low Light Intensity and in the Presence of Oxygen, *Macromolecules*, 2018, **51**(4), 1314–1324.
4 A. Kowalska, J. Sokolowski and K. Bociong, The Photoinitiators Used in Resin Based Dental Composite—A Review and Future Perspectives, *Polymers*, 2021, **13**(3), 470.
5 F. Marquardt, M. Bruns, H. Keul, Y. Yagci and M. Moller, Light-induced cross-linking and post-cross-linking modification of polyglycidol, *Chem. Commun.*, 2018, **54**(13), 1647–1650.
6 J. Li, Y. Hao, M. Zhong, L. Tang, J. Nie and X. Zhu, Synthesis of furan derivative as LED light photoinitiator: One-pot, low usage, photobleaching for light color 3D printing, *Dyes Pigm.*, 2019, **165**, 467–473.
7 H. K. Park, M. Shin, B. Kim, J. W. Park and H. Lee, A visible light-curable yet visible wavelength-transparent resin for stereolithography 3D printing, *NPG Asia Mater.*, 2018, **10**(4), 82–89.
8 P. Fiedor, M. Pilch, P. Szymaszek, A. Chachaj-Brekiesz, M. Galek and J. Ortyl, Photochemical Study of a New Bimolecular Photoinitiating System for Vat Photopolymerization 3D Printing Techniques under Visible Light, *Catalysts*, 2020, **10**(3), 284.
9 A. Bagheri and J. Jin, Photopolymerization in 3D Printing, *ACS Appl. Polym. Mater.*, 2019, **1**, 593–611.
10 M. Chen, M. Zhong and J. A. Johnson, Light-Controlled Radical Polymerization: Mechanisms, Methods, and Applications, *Chem. Rev.*, 2016, **116**(17), 10167–10211.
11 J. Tan, X. Dai, Y. Zhang, L. Yu, H. Sun and L. Zhang, Photoinitiated Polymerization-Induced Self-Assembly via Visible Light-Induced RAFT-Mediated Emulsion Polymerization, *ACS Macro Lett.*, 2019, **8**(2), 205–212.
12 X. Ma, D. Cao, X. Hu, J. Nie and T. Wang, Carbazolyl α-diketones as novel photoinitiators in photopolymerization under LEDs, *Prog. Org. Coat.*, 2020, **144**, 105651.
13 G. Sun, Y. Huang, J. Ma, D. Li, Q. Fan, Y. Li and J. Shao, Photoinitiation mechanisms and photogelation kinetics of blue light induced polymerization of acrylamide with bicomponent photoinitiators, *J. Polym. Sci.*, 2021, **59**(7), 567–577.
14 F. Dumur, Recent advances on benzylidene cyclopentanones as visible light photoinitiators of polymerization, *Eur. Polym. J.*, 2022, **181**, 111639.
15 K. Kaya, J. Kreutzer and Y. Yagci, Diphenylphenacyl sulfonium salt as dual photoinitiator for free radical and cationic polymerizations, *J. Polym. Sci., Part A: Polym. Chem.*, 2018, **56**(4), 451–457.
16 J. Li, J. Nie and X. Zhu, Hydrogen bond complex used as visible light photoinitiating system for free radical photopolymerization: Photobleaching, water solubility, *Prog. Org. Coat.*, 2021, **151**, 106099.
17 G. Noirbent and F. Dumur, Photoinitiators of polymerization with reduced environmental impact: Nature as an unlimited and renewable source of dyes, *Eur. Polym. J.*, 2021, **142**, 110109.
18 J. Zhao, J. Lalevée, H. Lu, R. MacQueen, S. H. Kable, T. W. Schmidt, M. H. Stenzel and P. Xiao, A new role of curcumin: as a multicolor photoinitiator for polymer fabrication under household UV to red LED bulbs, *Polym. Chem.*, 2015, **6**(28), 5053–5061.
19 P. Guinot, A. Gargadennec, P. La Fisca, A. Fruchier, C. Andary and L. Mondolot, Serratula tinctoria, a source of

natural dye: Flavonoid pattern and histolocalization, *Ind. Crops Prod.*, 2009, **29**(3), 320–325.
20 T. Maoka, Carotenoids as natural functional pigments, *J. Nat. Med.*, 2020, **74**(1), 1–16.
21 K. Phan, E. Van Den Broeck, V. Van Speybroeck, K. De Clerck, K. Raes and S. De Meester, The potential of anthocyanins from blueberries as a natural dye for cotton: A combined experimental and theoretical study, *Dyes Pigm.*, 2020, **176**, 108180.
22 F. Dumur, Recent advances on benzylidene ketones as photoinitiators of polymerization, *Eur. Polym. J.*, 2022, **178**, 111500.
23 M. Ibrahim-Ouali and F. Dumur, Recent advances on chalcone-based photoinitiators of polymerization, *Eur. Polym. J.*, 2021, **158**.
24 F. Zhang, Y. Luo, J. Song, X. Guo, W. Liu, C. Ma, Y. Huang, M. Ge, Z. Bo and Q. Meng, Triphenylamine-based dyes for dye-sensitized solar cells, *Dyes Pigm.*, 2009, **81**(3), 224–230.
25 X. Gan, Y. Wang, X. Ge, W. Li, X. Zhang, W. Zhu, H. Zhou, J. Wu and Y. Tian, Triphenylamine isophorone derivatives with two photon absorption: Photo-physical property, DFT study and bio-imaging, *Dyes Pigm.*, 2015, **120**, 65–73.
26 Y. N. Luponosov, A. N. Solodukhin and S. A. Ponomarenko, Branched triphenylamine-based oligomers for organic electronics, *Polym. Sci., Ser. C*, 2014, **56**(1), 104–134.
27 B. Yang, S. K. Kim, H. Xu, Y. I. Park, H. Zhang, C. Gu, F. Shen, C. Wang, D. Liu, X. Liu, M. Hanif, S. Tang, W. Li, F. Li, J. Shen, J. W. Park and Y. Ma, The origin of the improved efficiency and stability of triphenylamine-substituted anthracene derivatives for OLEDs: a theoretical investigation, *ChemPhysChem*, 2008, **9**(17), 2601–2609.
28 M. Jin, M. Yu, Y. Zhang, D. Wan and H. Pu, 2,2,2-trifluoroacetophenone-based D–π-A type photoinitiators for radical and cationic photopolymerizations under near-UV and visible LEDs, *J. Polym. Sci., Part A: Polym. Chem.*, 2016, **54**(13), 1945–1954.
29 S. Yao, H. Y. Ahn, X. Wang, J. Fu, E. W. Van Stryland, D. J. Hagan and K. D. Belfield, Donor-acceptor-donor fluorene derivatives for two-photon fluorescence lysosomal imaging, *J. Org. Chem.*, 2010, **75**(12), 3965–3974.
30 H. Chen, G. Noirbent, K. Sun, D. Brunel, D. Gigmes, F. Morlet-Savary, Y. Zhang, S. Liu, P. Xiao, F. Dumur and J. Lalevée, Photoinitiators derived from natural product scaffolds: monochalcones in three-component photoinitiating systems and their applications in 3D printing, *Polym. Chem.*, 2020, **11**(28), 4647–4659.
31 S. Chen, C. Qin, M. Jin, H. Pan and D. Wan, Novel chalcone derivatives with large conjugation structures as photosensitizers for versatile photopolymerization, *J. Polym. Sci.*, 2021, **59**(7), 578–593.
32 H. Fu, Y. Qiu, J. You, T. Hao, B. Fan, J. Nie and T. Wang, Photopolymerization of acrylate resin and ceramic suspensions with benzylidene ketones under blue/green LED, *Polymer*, 2019, **184**, 121841.
33 L. Deng and J. Qu, Synthesis and properties of novel bischalcone-based photoinitiators for LED polymerization with photobleaching and low migration, *Prog. Org. Coat.*, 2023, **174**, 107240.
34 F. Dumur, Recent Advances on Visible Light Metal-Based Photocatalysts for Polymerization under Low Light Intensity, *Catalysts*, 2019, **9**, 736.
35 M. Abdallah, D. Magaldi, A. Hijazi, B. Graff, F. Dumur, J. P. Fouassier, T. T. Bui, F. Goubard and J. Lalevée, Development of new high–performance visible light photoinitiators based on carbazole scaffold and their applications in 3d printing and photocomposite synthesis, *J. Polym. Sci., Part A: Polym. Chem.*, 2019, **57**(20), 2081–2092.
36 C. Pigot, G. Noirbent, T. T. Bui, S. Peralta, D. Gigmes, M. Nechab and F. Dumur, Push-Pull Chromophores Based on the Naphthalene Scaffold: Potential Candidates for Optoelectronic Applications, *Materials*, 2019, **12**(8), 1342.
37 H. Chen, G. Noirbent, Y. Zhang, D. Brunel, D. Gigmes, F. Morlet-Savary, B. Graff, P. Xiao, F. Dumur and J. Lalevée, Novel D–π-A and A–π-D–π-A three-component photoinitiating systems based on carbazole/triphenylamino based chalcones and application in 3D and 4D printing, *Polym. Chem.*, 2020, **11**(40), 6512–6528.
38 X. Ju, X. Hu, Y. Gao, J. Nie and F. Sun, Two hydrogen donor-containing naphthalimide benzyl thioether photoinitiators for LED photopolymerization, *Prog. Org. Coat.*, 2022, **162**, 106562.
39 M. Abdallah, H. Le, A. Hijazi, M. Schmitt, B. Graff, F. Dumur, T.-T. Bui, F. Goubard, J.-P. Fouassier and J. Lalevée, Acridone derivatives as high performance visible light photoinitiators for cationic and radical photosensitive resins for 3D printing technology and for low migration photopolymer property, *Polymer*, 2018, **159**, 47–58.
40 Y. Liu, T. Wang, C. Xie, X. Tian, L. Song, L. Liu, Z. Wang and Q. Yu, Naphthyl-based acylphosphine oxide photoinitiators with high effiency and low migration, *Prog. Org. Coat.*, 2020, **142**.
41 R. Nazir, P. Danilevicius, D. Gray, M. Farsari and D. T. Gryko, Push–Pull Acylo-Phosphine Oxides for Two-Photon-Induced Polymerization, *Macromolecules*, 2013, **46**(18), 7239–7244.
42 T. Xue, B. Huang, Y. Li, X. Li, J. Nie and X. Zhu, Enone dyes as visible photoinitiator in radical polymerization: The influence of peripheral N-alkylated (hetero)aromatic amine group, *J. Photochem. Photobiol., A*, 2021, **419**, 113449.
43 N. Giacoletto and F. Dumur, Recent Advances in bis-Chalcone-Based Photoinitiators of Polymerization: From Mechanistic Investigations to Applications, *Molecules*, 2021, **26**(11), 3192.

